JOURNAL OF MATERIALS SCIENCE 27 (1992) 3821–3826

# Interfacial stress state present in a "thin-slice" fibre push-out test

M. N. KALLAS, D. A. KOSS*, H. T. HAHN and J. R. HELLMANN*
*Department of Engineering Science and Mechanics, and *Department of Materials Science and Engineering, The Pennsylvania State University, University Park, PA 16802, USA*

An analysis of the stress distributions along the fibre–matrix interface in a "thin-slice" fibre push-out test is presented for selected test geometries. For the small specimen thicknesses often required to displace large-diameter fibres with high interfacial shear strengths, finite element analysis indicates that large bending stresses may be present. The magnitude of these stresses and their spatial distribution can be very sensitive to the test configuration. For certain test geometries, the specimen configuration itself may alter the interfacial failure process from one which initiates due to a maximum in shear stress near the top surface adjacent to the indentor, to one which involves mixed mode crack growth up from the bottom surface and/or yielding within the matrix near the interface.

## 1. Introduction

Since its introduction as a method of measuring matrix–fibre frictional stresses in ceramic composites, the fibre "push-out" (or "push-through") test has been used extensively in the ceramic matrix composite (CMC) studies [1]. In its original form, the test involved the use of an indentor to push a small diameter fibre ($\approx$20–30 μm) into a composite specimen with a thickness of several millimetres. In such cases, the sliding distances along which the fibre–matrix shear displacements occur are smaller than the specimen thickness. Furthermore, in this "thick-specimen" configuration, failure of the interface initiates at/or near the top surface, close to the indentor, where the local shear stress is a maximum [1–7]. Based on the associated load–displacement response as the fibre is pushed into the specimen, several analyses have been proposed for interpreting the observed data in terms of the interfacial shear strength, residual clamping stresses, and a calculated coefficient of friction [3–8].

Recently, considerable interest has been generated in the interfacial characteristics of both metal matrix composites (MMCs) and intermetallic matrix composites (IMCs). This interest is due to the realization of the important role that an interface plays in controlling the overall composite strength and toughness. However, there are two important differences between interfacial shear strength testing of CMCs and either MMCs or IMCs. Firstly, even without a chemical bond at the interface, the large thermally induced clamping stresses result in frictional stresses in the MMCs or IMCs which are usually an order of magnitude higher than in CMCs [9, 10]. Secondly, the fibres of choice in MMCs or IMCs, usually SiC or single-crystal sapphire, have diameters which are often a factor of five to ten times larger than those typically used in CMCs. The result is that large loads are required to displace the fibres in thick specimens. This causes experimental problems: either the fibre is damaged during loading, especially with a diamond pyramid indentor, or the flat-bottomed indentor, often a small cylinder of tungsten carbide, fails prior to any measurable fibre displacement.

Given the above difficulties, the most common experimental technique to study the interfacial strength properties of MMCs and IMCs is to utilize a "thin-slice" fibre push-out specimen [9–13], as shown in Fig. 1. In this case, the test specimen is sufficiently thin (usually less than 1 mm) to enable the entire length of fibre to slide out of the matrix. To allow unrestrained fibre motion, the specimen is usually supported by a plate with a hole or slot that is concentrically located with respect to the fibre. In many cases, neither the width of the slot/hole nor thickness of the specimen is reported.

The purpose of this study was to present the results of a finite element computational simulation of the thin-slice push-out test of a typical metal matrix composite. Of significance is the observation that large normal stresses can be induced at the fibre–matrix interface at the bottom surface of the specimen. These normal stresses can alter the interfacial failure process such that rather than interfacial failure initiating near the upper surface of the specimen adjacent to the indentor, failure can initiate by crack nucleation along the fibre–matrix interface at the bottom surface of the specimen and/or by matrix yielding along the interface. Interpretation of the observed load–time or load–displacement data will be quite different as a result.

## 2. Finite element procedure

An axisymmetric finite element (FE) model has been developed to emulate a fibre push-out specimen and test apparatus as shown in Fig. 1. The analysis

0022–2461  

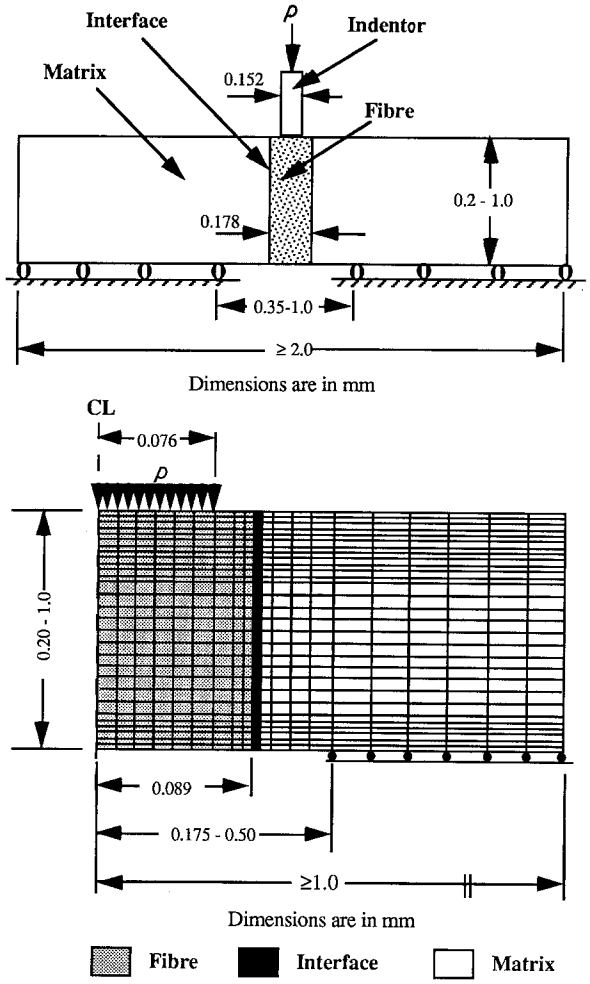


*Figure 1* A schematic illustration of a "thin-slice" fibre push-out test and the associated axisymmetric finite element model.

presented in this paper accounts for matrix yielding, which may occur in very thin specimens, and post-yielding behaviour. The element used for this analysis is a two-dimensional isoparametric element (ANSYS code) which has the capability of axisymmetric analysis. The geometry of the model, loading arrangement, and boundary conditions are selected to represent those of the actual experimental technique. The model has the capability of simulating an interfacial layer between the fibre and the matrix. However, the material used in the present analysis (niobium/sapphire MMC) has been shown [14] to exhibit a significant degree of chemical bonding between the fibre and matrix materials. Niobium–sapphire is convenient model system because of the very good match of thermal expansion coefficients and the resulting small residual thermoelastic stresses, which we ignore in the present illustration. Therefore, the interfacial layer will be given the same material properties as the niobium matrix. It follows that perfect bonding conditions exist along the interface, and therefore the model applies only to those loads less than those at which interfacial debonding starts to occur. In those MMCs which do not exhibit a chemical bond between the fibre and matrix, thermoelastic clamping will maintain registry between the matrix and fibre until the applied load initiates debonding by shear; the present analysis should be applicable to that load.

The present analysis examines the mechanically induced stresses due to the imposed loads which are exerted on the inner part of the fibre by the flat indentor. Several push-out specimen geometries, within the limits shown in Fig. 1, are examined to evaluate the effect of specimen configuration on the interfacial failure modes observed experimentally. In all cases, the specimen is supported by a thick, rigid plate with a hole whose diameter is variable; the fibre is always concentrically located with respect to the hole.

## 3. Results and discussion

The results of the FE analysis are based on elastic behaviour of 152 μm diameter sapphire filaments ($E$ = 379 GPa and $\nu$ = 0.22) embedded in a niobium matrix ($E$ = 95 GPa, $\nu$ = 0.29 and $\sigma_y$ = 190 MPa) whose stress–strain behaviour can be described as bilinear kinematic hardening. The circular support hole was varied between 0.35 and 1.00 mm diameter, while specimen thickness ranged from 0.2–1.5 mm. In order to compare the stress distributions of different test geometries, the normalized (with respect to indentor pressure) interfacial stress components are plotted as a function of the normalized (with respect to specimen thickness) position along the interface. Stresses due to differences in the coefficients of thermal expansion (ΔCTE effects) are ignored. The indentor pressure, $p$, is defined here as the external load, $P$, on the indentor divided by the indentor cross-sectional area ($\pi r_i^2$) with $r_i$ = 76 μm. In the analysis of the specimen geometry, two important parameters are examined: (i) specimen thickness, and (ii) support hole size. The role that each parameter plays in the interfacial failure process will be discussed below.

### 3.1. Effect of specimen thickness

Selection of an appropriate specimen thickness for a "thin-slice" fibre push-out test must be based on variables such as the existence of a chemical bond and/or thermoelastic clamping between the fibre and the matrix, fibre surface quality, matrix stiffness, and matrix strength. Using the niobium/sapphire composite as a model system, Fig. 2 shows the effect of specimen thickness on the interfacial shear and radial stress distributions. For clarity, only two geometries are selected and depicted in Fig. 2 to demonstrate the predicted effect of specimen thickness on the interfacial stress state.

As noted in Fig. 2a and predicted previously for "thick-slice" fibre-push-out configurations [3–8], the shear stress $S_{rz}$ at the interface is not uniform along the fibre length. For the thin-slice specimens in Figs 2 and 3, $S_{rz}$ has a maximum value of 0.12–0.13$p$, where $p$ is the applied indentor pressure, at a location of 0.05$t$–0.10$t$, where $t$ is specimen thickness, below the top surface of the specimen. Owing to the shear stress distribution, failure of the fibre–matrix interface can initiate by a shear mechanism at the point of maximum shear stress near the top of the specimen, and propagate towards the bottom of the specimen. This is the generally assumed interfacial failure sequence for

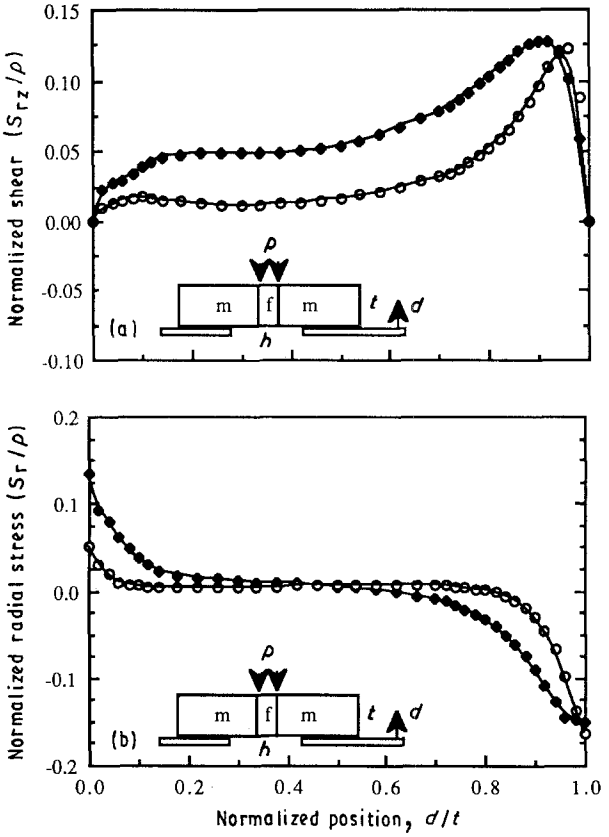


*Figure 2* Effect of specimen thickness on (a) the shear stress distribution, and (b) the radial stress distribution at the F/M interface of a niobium/sapphire composite. (◆) $t = 0.50$ mm, $h = 0.35$ mm; (○) $t = 1.00$ mm, $h = 0.35$ mm.

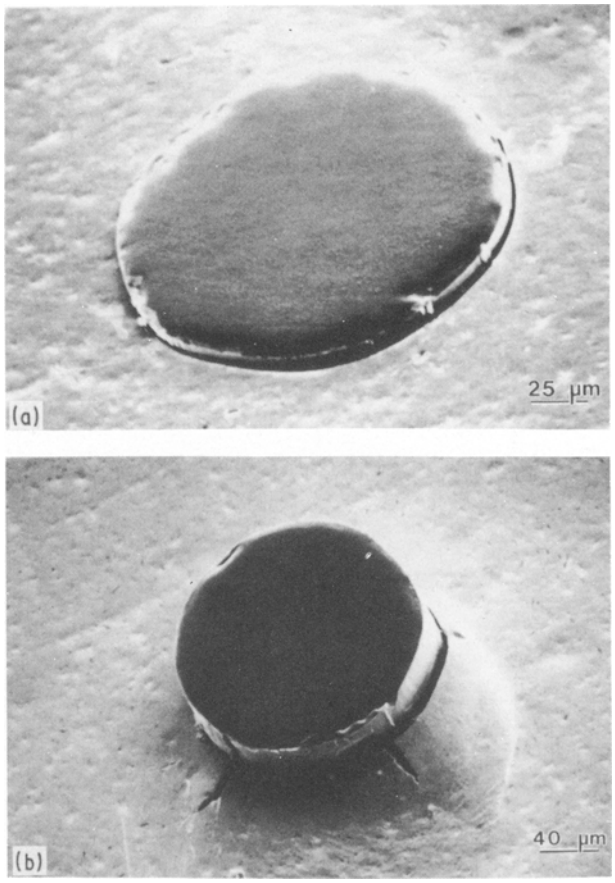


*Figure 3* Optical micrograph of a niobium/sapphire thin-slice push-out specimen showing (a) radial displacements and crack initiation at the bottom surface of the specimen, and (b) radial cracks within the matrix near the fibre–matrix interface of a pushed out fibre.

push-out or push-through tests, especially for CMCs where the matrix has a high stiffness and interfaces tend to exhibit smaller shear strengths than in MMCs.

In contrast, for thin-slice specimens the conventional interpretation of the above failure sequence may not be correct. Fig. 2b shows that a significant radial stress component, $S_r$, exists at the bottom of the niobium–sapphire interface. A result of an axisymmetrical bending, the $S_r$ is tensile and its magnitude approaches $0.14p$ for a 0.5 mm thick specimen. Even though most MMCs and IMCs are characterized by residual compressive stresses due to a thermal expansion mismatch between the fibre and matrix, the mechanical bending stresses may exceed the thermally induced stresses during loading. Fig. 2b indicates that, unlike the stress state in the thicker specimen ($t = 1$ mm), the presence of large tensile stresses in thin specimens can result in crack initiation at the bottom interface rather than shear failure initiating near the top surface of the specimen. Subsequent crack growth will likely occur in a mixed mode I and II manner with mode I dominating initially, but an increasing mode II component as the crack propagates. This is indicated by a comparison of stresses in Fig. 2; it should be noted that the stress state does not take into account the presence of an interfacial crack.

The above failure sequence has been observed experimentally. Fig. 3a shows the bottom surface of a specimen of $t = 0.5$ mm and $h = 0.35$ mm prior to interfacial shear at the top surface. Crack initiation is manifested by the existence of a circumferential crack and permanent plastic radial deformation in the matrix material. For the case shown in Fig. 3a, the load at which the fibre–matrix interface failed by a crack initiation corresponds to a radial stress that is higher than the debond strength, $\sigma_d$, of a niobium–sapphire interface: $\sigma_d \simeq 87$ MPa [15].

Mode I interfacial failure is also shown in Fig. 3b, except that circumferential as well as radial cracks are produced in this case. This specimen had a thickness of 0.2 mm and the diameter of the supporting hole was 0.35 mm, thus producing large tensile stress, beyond yielding stress, in the matrix in the radial as well as the hoop direction. The distributions of these stresses, shown in Fig. 4, are based on a bilinear kinematic hardening behaviour of the niobium matrix. It is evident from Fig. 4 that the magnitude of the stresses, due to the applied load of 16.5 N, are well beyond the yield strength of niobium ($\sigma_y \simeq 190$ MPa) and consistent with the plasticity evident in the matrix [13]. Shear stress distribution shown in Fig. 4a indicates matrix yielding over most of the interfacial region, as demonstrated on the surface of the pushed fibre in Fig. 3b. Matrix yielding is believed to have resulted in blunting interfacial crack propagation by shear. We also note that in order for the normally ductile niobium to exhibit radial cracking, large tensile hoop stresses, as shown in Fig. 4b, are indeed present.

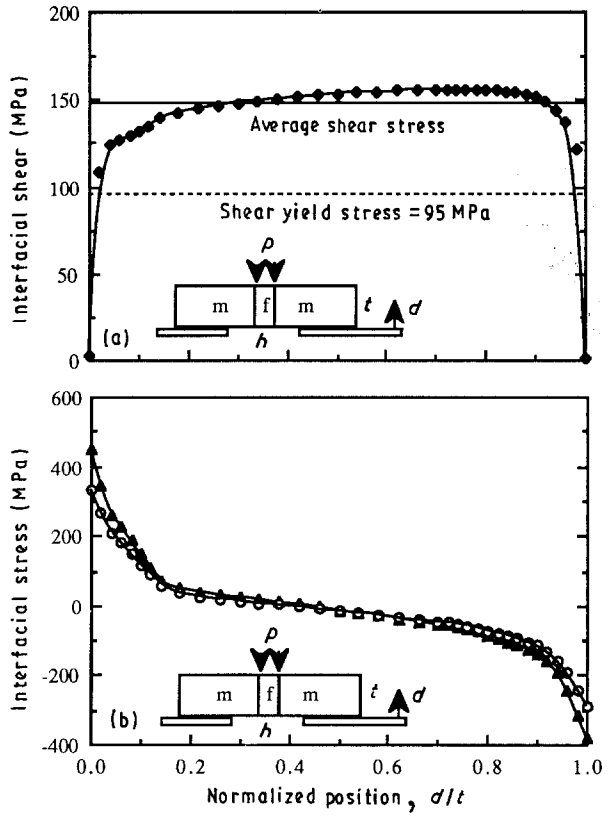


*Figure 4* (a) Interfacial shear stress distribution, and (b) (▲) radial and (○) hoop stress distributions in a thin niobium/sapphire specimen with $t = 0.20$ mm and $h = 0.35$ mm. The average shear stress on the specimen due to an applied load of 16.5 N and the niobium shear yield stress are also shown.

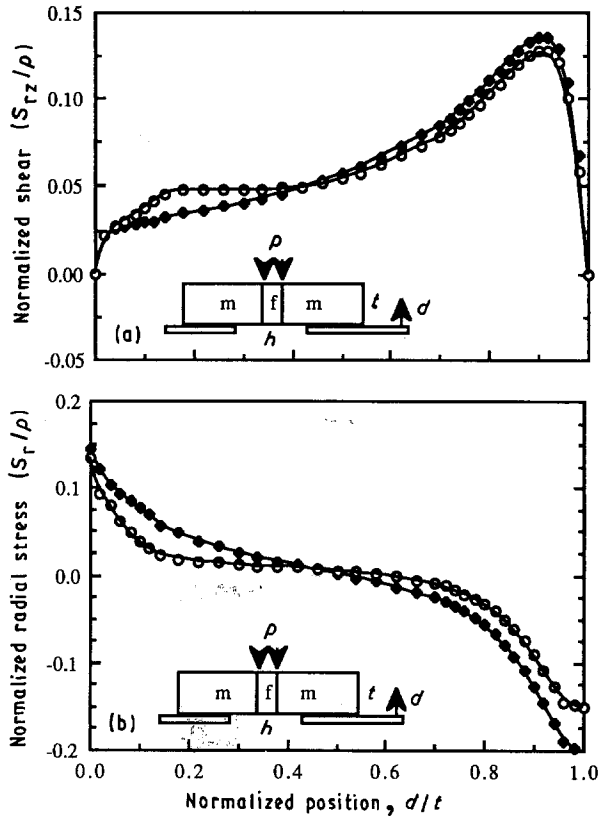


*Figure 5* Effect of support hole size on (a) the shear stress distribution, and (b) the radial stress distributions at the fibre–matrix interface of a niobium/sapphire composite. (◆) $t = 0.50$ mm, $h = 1.00$ mm; (○) $t = 0.50$ mm, $h = 0.35$ mm.

## 3.2. Effect of support hole size

The effect of the support hole size, $h$, on the interfacial stress state of the specimen is shown in Fig. 5. While hole size has a minor effect on the magnitude of the maximum stresses, it clearly alters the distribution of interfacial stresses. Examining Fig. 5 reveals that as $h$ increases at a given specimen thickness, the radial tensile stress over the bottom interfacial region also increases. Also, one can observe that near the top of the specimen ($0.5 \leqslant d/t \leqslant 1$) the compressive radial stress component, which is a result of bending, increases with increasing $h$. This results in a larger shear stress component sustained by the specimen near the indentor.

## 3.3. Combined effects of specimen thickness and support hole size

The effects of specimen geometry changes, wherein both specimen thickness and hole size change, cause a significant redistribution of stress components along the fibre–matrix interface. As shown in Fig. 6, this has significant effects on the von Mises equivalent stress, $\bar{\sigma}$. For thick specimens supported over a small hole, $\bar{\sigma}$ mimics the interfacial shear stress, $\sigma_{rz}$, in Fig. 2a with a pronounced maximum near the indentor. However, for thin specimens supported over a relatively large hole, $\bar{\sigma}$ is very large over nearly the entire length of fibre–matrix interface. For a MMC, with a strong interfacial bond, Fig. 6 suggests a failure process in a thin-slice push-out test which may be a function of specimen configuration. Specifically, thick specimens may fail by interfacial shear initiating near the top surface, as expected. However, due to the large value of $\bar{\sigma}$, thin specimens supported over a large hole/slot may fail by matrix yielding near the interface along most the length of the fibre, even at locations where $\sigma_{rz}$ is small. This is an important alternative to "interfacial shear" due solely to large $\sigma_{rz}$ values.

Fig. 7 summarizes the effects of specimen geometry on the interfacial stresses during a "thin-slice" fibre

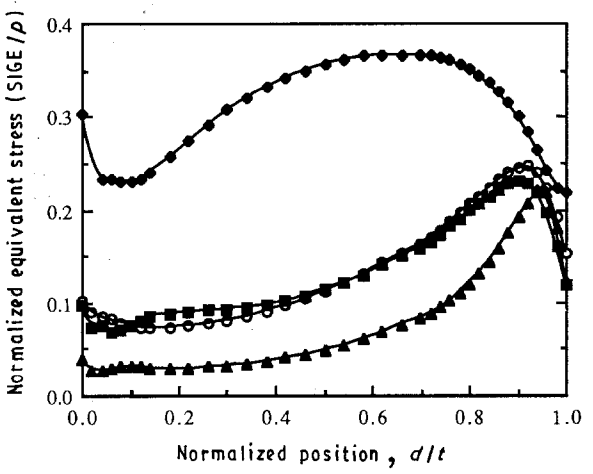


*Figure 6* Equivalent (von Mises) stress distribution at the interface of thin-slice push-out specimens of variable geometries. (◆) $t = 0.20$ mm, $h = 0.35$ mm; (○) $t = 0.50$ mm, $h = 1.00$ mm; (▲) $t = 1.00$ mm, $h = 0.35$ mm; (■) $t = 0.50$ mm, $h = 0.35$ mm.

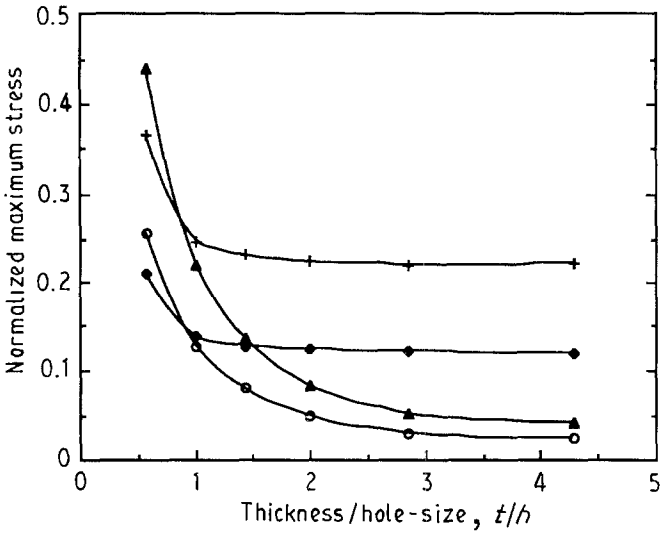


*Figure 7* Summary of specimen geometry effect on the maximum interfacial stress components. Graph shows the normalized (with respect to indentor pressure $p$) maximum stress components versus thickness/hole size ratio, $t/h$. (▲) Radial stress, (◆) shear stress, (○) hp stress, ( + ) equivalent stress.

push-out test. Shown in Fig. 7 are the maximum stresses as a function of thickness-to-span ratio, $t/h$. It is interesting to observe that the maximum shear stress is almost independent of specimen geometry for $t/h \geqslant 1$. However, the figure clearly shows the strong dependence on specimen geometry of maximum tensile stress in the radial and hoop directions. Fig. 7 also implies that one could force a nearly pure shear failure (dictated by $\sigma_{rz}$) by maximizing specimen thickness and keeping the hole size at a minimum. While this might be a valid description of interfacial failure when dealing with weak interfaces such as in CMCs, the case can be quite different for MMCs. For example, as described above, localized matrix yielding may precede interfacial failure due to the large magnitude of $\bar{\sigma}$. Furthermore, a large radial stress at the fibre–matrix interface may cause interfacial debonding and mixed mode crack growth as observed in Fig. 3. Thus, while researchers have resorted to thinner specimens in order to successfully shear a well-bonded fibre out of the matrix, the test configuration may introduce other possible failure mechanisms due to the high tensile radial and hoop stresses as well as large equivalent shear stresses within the matrix (see Figs 6 and 7). This case is clearly shown in Fig. 7 for specimens with $t/h < 1$. Therefore, considerable care must be exercised not only in interpreting the test data but also in configuring the initial test. The above also indicates the crudeness of using the average shear stress as an interfacial shear strength. Such data may be very misleading, especially if obtained from thin-slice specimens ($t/h < 1$) of varying $t/h$ values.

## 4. Conclusion

The stress distributions along the fibre–matrix interface in a thin-slice fibre push-out specimen are shown to depend on specimen geometry. In particular, significant bending stresses can be present in thin-slice push-out specimens of a composite that has a high interfacial strength, such as in MMCs. The bending stresses consist of both radial and hoop components whose magnitude depend on both specimen thickness and support hole size. As a result, the interfacial failure process in thin-slice push-out tests depends on push-out test geometries. Specifically, interfacial failure may involve (1) an interfacial shear process initiating near the indentor, which is normally assumed, (2) mixed mode I/mode II crack growth initiating at the bottom fibre–matrix interface opposite the indentor, or (3) matrix yielding even under conditions of a small interfacial shear stress but large equivalent stress. Interpretation of the test data in terms of an "interfacial shear strength" is thus complicated by a variable multiaxial failure processes. At best, reliable comparative results may be made using thin-slice push-out tests while adhering to constant specimen thickness-to-hole size ratio of greater than two (Fig. 7). At worst, unspecified and probably large support hole sizes render reported data useless.

## Acknowledgements

The authors acknowledge the support of NASA through Grant no. NAGW-1381 and the Cooperative Program in High Temperature Engineering Materials Research within the Centre for Advanced Materials at The Pennsylvania State University.

## References

1. D. B. MARSHALL, *J. Amer. Ceram. Soc.* **67** (1984) C-259.
2. K. T. FABER, S. H. ADVANI, J. K. LEE and J. T. LIN, *ibid.* **69** (1986) C208.
3. D. B. MARSHALL and W. C. OLIVER, *ibid.* **70** (1987) 542.
4. D. H. GRANDE, J. F. MANDELL and K. C. C. HONG, *J. Mater. Sci* **23** (1988) 311.
5. J. D. BRIGHT, D. K. SHETTY, C. W. GRIFFIOR and S. Y. LIMAYE, *J. Amer. Ceram. Soc.* **72** (1989) 1891.
6. C. H. HSUCH, *Acta Metall. Mater.* **38** (1990) 406.
7. R. J. KERANS, P. D. JERO, T. A. PARTHASARATHY and A. CHETTERJEE, in "Intermetallic Matrix Composites" edited by D. L. Antan, P. L. Martin, D. B. Miracle and R. McMeeking (MRS, Pittsburgh) (1990) p. 263.
8. S. K. MITAL and C. C. CHAMIS, unpublished research (1990).
9. R. D. NOEBE, R. R. BOWMAN and J. E. ELDRIDGE, in "Intermetallic Matrix Composites" edited by D. L. Antan, P. L. Martin, D. B. Miracle and R. McMeeking (MRS, Pittsburgh) (1990) p. 323.

10. C. A. MOOSE, D. A. KOSS and J. R. HELLMANN, *ibid.*
11. J. W. LAUGHER, N. J. SHAW, R. T. BHATT and J. A. DI CARLO, *Ceram. Engng Sci. Proc.* **7** (1986) 7.
12. M. K. BRUN and R. N. SINGH, *Adv. Ceram. Mater.* **3** (1988) 506.
13. R. PETRICH, D. A. KOSS and J. R. HELLMANN and M. N. KALLAS, in "Interfacial Phenomena in Composite Materials '91", edited by I. Verpoest and F. Jones (Butterworth-Heineman, Oxford, 1991) p. 155.
14. S. MOROZUMI, M. KIKUCHI and T. NISHINO, *J. Mater. Sci.* **16** (1981) 2137.
15. M. G. STOUT, M. L. LOVATO, A. G. ZOCCO and T. R JERVIS, Los Alamos Laboratory, LA-11815-ms (1990).

*Received 21 March*
*and accepted 1 July 1991*